Distant Dipolar Fields in Laser-Polarized Gases on Macroscopic Scales

Paul P. Zänker, Jörg Schmiedeskamp, and Hans W. Spiess[*]
Max Planck Institute for Polymer Research, Ackermannweg 10, 55128 Mainz, Germany

Rodolfo H. Acosta
LANAIS RMS–Facultad de Matemática, Astronomía, y Física–Universidad Nacional de Córdoba, Ciudad Universitaria, X5016LAE Córdoba, Argentina

(Received 5 December 2007; published 29 May 2008)

Distant dipolar fields among nuclear spins on macroscopic scales in the gas phase are reported for the first time. Their observation via interatomic multiple quantum coherences requires high nuclear spin polarization corresponding to spin temperatures of a few mK, which is generated in laser-polarized ^{3}He, and proper control of the gas diffusion through a heavier buffer gas. This combination of physics at low and ambient temperatures opens up new ways of studying the relative translational diffusion of atoms and of gas diffusion in structures with a large range of length scales.

DOI: 10.1103/PhysRevLett.100.213001 PACS numbers: 33.40.+f, 33.25.+k, 82.56.Lz

Dipole-dipole coupling is one of the basic interactions in physics. As far as nuclear magnetic resonance (NMR) is concerned, it is mostly observed and exploited to study structure and dynamics on the molecular level. More than 10 years ago, however, it was shown that dipole-dipole coupling between nuclear spins in liquids can also arise from distant dipolar fields (DDFs) and can be detected by intermolecular multiple quantum coherences (IMQCs) [1,2]. The progress in understanding their physical basis [3,4] led to the development of important applications in different fields, ranging from physics to medicine [5–9]. As on the molecular scale, spectroscopic observation of DDFs requires that the dipolar coupled species retain their distance and orientation over sufficiently long times [10,11]. As spatial diffusion in gases is orders of magnitudes faster than in condensed phases, this requirement is usually violated in the gas phase and DDFs have not yet been observed in a gas at ambient pressures. If this problem can be overcome, however, the rapid diffusion in gases can be exploited to probe such DDFs over much larger spatial excursions on macroscopic length scales, e.g., in porous media or in imaging. Along these lines, dipole couplings between gas filled nanovoids at pressures in the kbar regime were indirectly detected by Baugh *et al.* using H_2 [12], and IMQCs between gas and liquid phase were observed by Granwehr *et al.* using laser-polarized (LP) ^{129}Xe and ^{1}He [8]. The observation of DDFs in gases themselves, however, is also hampered by the low spin density leading to low magnetizations even in strong magnetic fields. As we show below, these problems can be solved by using LP noble gases with nuclear spin polarizations corresponding to spin temperatures of a few mK and controlling the diffusion coefficient by admixing heavy buffer gases [13,14]. Using this strategy the first signals of IMQCs in the gas phase itself are presented here.

Intermolecular MQCs were first detected by the observation of unexpected cross-peaks in two-dimensional spectra, corresponding to coherences between independent molecules in solution [1,2]. These cross-peaks were measured with the correlation spectroscopy revamped by an asymmetric z-gradient echo detection (CRAZED) experiment, shown in Fig. 1, where two gradient pulses with a ratio of 1:n act as an n-quantum filter. Similar to a spin echo sequence [15], the excitation radio frequency (rf) pulse has a flip angle of 90°, while the flip angle β of the refocusing pulse has an optimum value for different n-quantum coherences, for instance $\beta = 120°$ for double-quantum coherences (DQC) [16]. In contrast to single-quantum (SQ) signals which decay from a maximum value, IMQC signals typically build up from zero, peak out, and decay with an oscillation [17]. Two different pictures were proposed to explain the occurrence of IMQCs. The classical picture describes the effect by a DDF, which is generated by the magnetization of one spin component, and acts on the evolution of the magnetization of another spin component [4]. The quantum-mechanical approach, introduced by Warren and coworkers [1–3,18–20], is described shortly in the following.

Here, a density matrix picture is employed, which explicitly retains dipolar couplings between distant pairs of spins and removes the usual truncation of the density matrix ρ_{eq} in the "high temperature approximation." For

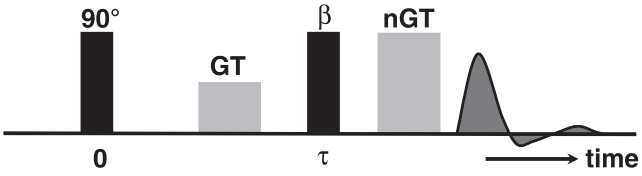

FIG. 1. Standard n-quantum CRAZED sequence. The pulses are delayed by time τ and the area of the second gradient pulse is n times larger than the first one and acts as a filter for n-quantum coherences. The flip angle β of the second pulse must be optimized for each value of n.

N spins $I = 1/2$ in an external magnetic field B_0, the equilibrium density matrix is obtained by taking the product of the equilibrium density matrices of all individual spins of the sample as

$$\rho_{\mathrm{eq}} = 2^{-N}\prod_i(\mathbf{1} - \mathcal{J}I_{zi}), \tag{1}$$

where

$$\mathcal{J} = 2\tanh\left(\frac{\gamma\hbar B_0}{2kT}\right), \tag{2}$$

with γ the magnetogyric ratio of the nucleus, k the Boltzmann factor, and T the temperature of the sample. The factor $\mathcal{J}$ is directly related to the polarization of the system by $\mathcal{J} = 2P$, with $P = (p_+ - p_-)/(p_+ + p_-)$, where p_+ and p_- are the numbers of spins in the $m_I = 1/2$ and $m_I = -1/2$ states, respectively. Note that the factor $\mathcal{J}$ approaches $\gamma\hbar B_0/kT$ as the temperature increases, which means that the high temperature approximation is recovered for first order terms of Eq. (1). The observation of IMQCs is facilitated in systems with low effective spin temperature, because the higher order terms in the density matrix are precisely the ones that account for the presence of MQCs. For instance, first order terms of the form $\mathcal{J}^2\sum_{i\neq j}I_{zi}I_{zj}$ are rotated into $\mathcal{J}^2\sum_{i\neq j}I_{xi}I_{xj}$ by the application of the first rf pulse, and will lead to double-quantum signals in the detection period. Even though the factor $\mathcal{J}^2$ is about 4 orders of magnitude smaller than $\mathcal{J}$ in a sample of water at high magnetic fields, the high number of second order terms that contribute is large enough to make the signals observable [3]. For the particular case of LP ^{3}He, the system is driven out of equilibrium by a laser excitation of the electronic spin population which is subsequently transferred to the nuclear spins. Today, polarizations of 60% are routinely obtained for ^{3}He [21], independent of the external magnetic field in which experiments are performed. These polarizations correspond to low spin temperatures around 5 mK for fields of 4.7 T used in our experiments below. This in turn will considerably enhance the effect of $\mathcal{J}^n$ terms as compared with thermally polarized gases.

Another aspect that circumvents the occurrence of IMQCs in thermally polarized gases is the time where the signal maximum occurs. For the double-quantum signals considered in this Letter, this time is given by

$$t_{\max} \sim 2.2/(\mu_0\gamma M_0) = 2.2\tau_d, \tag{3}$$

where τ_d is referred to as the dipolar demagnetizing time and μ_0 is the vacuum permeability [1]. M_0 is the sample magnetization, which includes not only the polarization but also the spin density. In order to observe IDQC signals the relaxation times of the spins have to be at least on the order of $t_{\max}$. For thermal magnetizations, $t_{\max}$ is in the range of minutes, which therefore renders the detection of IDQCs virtually impossible. For LP gases, on the other hand, $t_{\max}$ is in the range of ms, and the demagnetizing time can be controlled by the polarization itself.

Therefore, IMQCs in gases can only build up and be detected in LP systems. This is a fundamental difference to most other applications of LP gases, where the large polarization is only needed for enhancing the signal to noise ratio of the measurements. However, a major drawback of this approach is that the polarization of the spins is not renewable, i.e., after a saturation rf pulse the spin system relaxes back to the small thermal polarization. This obstacle is overcome with an automated setup that permits the evacuation, refilling, and mixing of different gases in a sample cell located in a fixed position in the bore of the magnet, similar to the one described in [14].

As the calibration of the pulse flip angles is crucial for the experiments and reproducibility must be guaranteed, we first of all checked our setup with a nutation experiment. Measurements were carried out in a magnetic field of 4.7 T using a birdcage coil of 25 mm diameter. For each data point two spectra were acquired: the first one with a constant small flip angle of about 1° as a measure for the relative polarization, and the second one with a variable pulse length. The signal amplitude of the second spectrum was normalized by the amplitude of the first one. As T_1 relaxation times of ^{3}He were in the range of 10 min, the measurements are not time critical and up to eight calibration values were measured for each gas portion, depending on the used rf pulses. An example of a nutation spectrum recorded in LP ^{3}He is shown in Fig. 2, where t_p is the variable pulse length, yielding a 180° pulse of 70 μs. The symmetry of the curve around 180° ensures that radiation damping was effectively avoided [22]. In order to ensure that the DDF arises solely from the modulation introduced by the field gradients and is not influenced by the sample geometry, a spherical glass cell of 15 mm outer diameter was used as a sample container.

Finally, the effects of gas diffusion must be taken into account. For unrestricted ^{3}He at 1 bar the diffusion coefficient $D = 1.85$ cm^2/s is 5 orders of magnitude larger

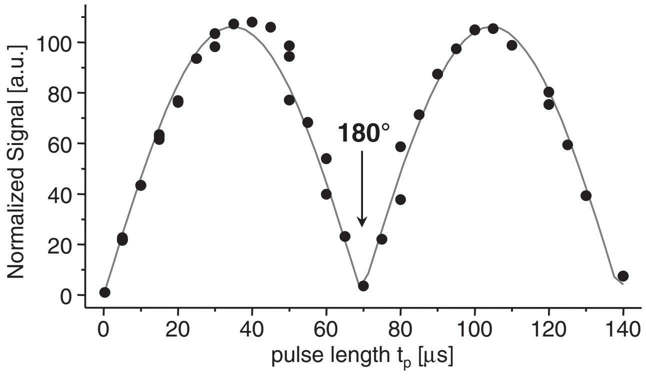

FIG. 2. Flip angle calibration measurements in LP ^{3}He. The normalized signal maximum values are plotted versus the rf pulse length. The line shows the fitted calibration curve.

than for bulk water. Therefore, suppressing diffusion is crucial for the detection of echo signals in gases, especially for long echo times. According to Eq. (3) the IDQC signal in LP ^{3}He gas at 1 bar and a polarization of 60% reaches its maximum at about 53 ms after the second rf pulse. This signal is additionally suppressed by T_2^* relaxation due to magnetic field inhomogeneities, for the present conditions with a time constant of about 14 ms. The diffusion coefficient of ^{3}He can be lowered by admixture with a heavier buffer gas such as SF_6 [14] and also by increasing the total pressure in the gas sample. As the estimated motional correlation time for echo signals in a mixture of 1 bar ^{3}He and 2 bar SF_6 is already in the order of 20 ms [23], it should be possible to suppress the effect of diffusion well enough to detect the rising slope of the IDQC signal. Therefore, in the following experiments, the diffusion coefficient was lowered by mixing 1 bar of LP ^{3}He with 6, 3, and 1 bar of SF_6, respectively, resulting in diffusion coefficients of $D = 0.09$, 0.21, and 0.95 cm^2/s, respectively.

The measurements of IDQCs in ^{3}He were performed using a CRAZED sequence with the following settings: 90° pulse 35 μs, pulse delay time $\tau = 600$ μs, first gradient pulse of duration 300 μs, and 30 mT/m. For these settings the correlation distance $d_c = \pi/(\gamma G T)$, which defines the length scale of the major contribution to the distant dipolar field [18], is 1.7 mm. This is about 1 to 2 orders of magnitude larger than typical values in liquids [9]. In order to minimize the loss of signal by diffusion suppression during the gradient pulses, the timings were chosen as short as possible. For such short durations, the impedance of the gradient coils delays the buildup of the currents, which leads to a deviation between the adjusted gradient parameters and the real gradient amplitudes. The second gradient pulse intensity was therefore calibrated by inspection of the SQ signal during the gradient and set in such a way that the echo was formed at the center of the pulse. A four-step phase cycle with $(x, y, -x, -y)$ for the first pulse and $(x, -x, x, -x)$ for the receiver was implemented to suppress the remaining SQ signals. Note that each phase cycling step is a separate experiment with a new gas mixture, requiring about 1 min. The four different phase step experiments are measured consecutively and automatically controlled by the spectrometer PC. The results are added up later during data processing to give the IDQC signal. This approach assures that no SQ signal is passing the DQ filter of the sequence.

The IDQC signal is acquired directly after the second gradient pulse. The magnitude of the resulting sum of the four different phase steps is shown in Fig. 3 for different gas mixtures. While the remaining SQ signal, which is present for small times in a single scan, is averaged out almost completely by the phase cycle, the sum of the signal builds up from zero, with the amplitude clearly exceeding the noise level for the two slower diffusion coefficients. The signal for $D = 0.09$ cm^2/s reaches its absolute maximum at a time of about 10 ms after the gradient pulse which is less than the predicted 53 ms, because T_2^* relaxation suppresses a further buildup. With increasing D the signal is further suppressed and the maximum shifts to shorter times. This effect was already exploited in order to measure D and T_2 simultaneously [24]. The maximum of the signal results from a competition between diffusion and relaxation and, neglecting spin-lattice relaxation, was shown to occur at $t_m = \ln(2Dk^2T_2 + 1)/2Dk^2$, with $k = \gamma G \delta$, and δ the gradient pulse duration. For the present experiments, and replacing T_2 by T_2^* the signal maximum times of 10, 8, and 4 ms are obtained for increasing D, which is in good agreement with our experimental data. The shifts and distortions of the signal result from echo formation in presence of rapid diffusion in the inhomogeneous field, as recently described in [13]. This relaxation attenuation can be reduced by performing a 2D version of the CRAZED sequence [17].

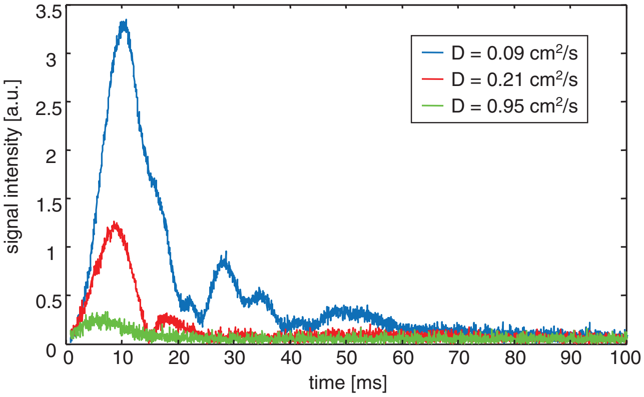

FIG. 3 (color). Magnitude signals of the CRAZED experiment in LP ^{3}He for different diffusion coefficients. The partial pressure of ^{3}He in the gas mixture is 1 bar for all measurements. The different colors correspond to different SF_6 partial pressures. Blue: 6 bar, $D = 0.09$ cm^2/s; red: 3 bar, $D = 0.21$ cm^2/s; green: 1 bar, $D = 0.95$ cm^2/s.

In order to verify the authenticity of the IDQC signal in LP ^{3}He, the dependence on the second rf pulse flip angle was checked. As already stated, this signal should display a maximum for $\beta = 120°$ [16]. Figure 4 shows the signal intensities of a set of CRAZED experiments with varying β in a gas mixture containing 1 bar ^{3}He and 6 bar SF_6. The experimental points clearly follow the plotted line of the theoretical relative signal amplitude function $f(\beta) = \sin\beta(1 - \cos\beta)$ [16] and strongest amplitudes clearly arise for $\beta = 120°$. The signal vanishes for $\beta = 180°$ showing that no SQ signal is present in the detection period. These measurements represent, to the best of our knowledge, the first experimental evidence of IDQC in the bulk gas phase, arising from the DDF in LP ^{3}He.

The ability to detect DDFs of nuclear spins in LP gases and their high sensitivity to diffusion and spatial restric-

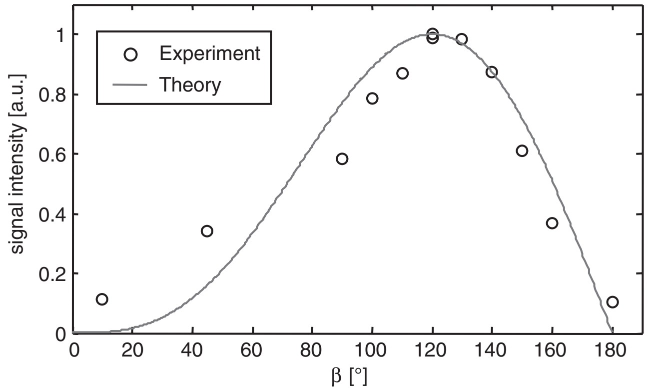

FIG. 4. Dependence of the measured CRAZED signal intensity on the flip angle of the second rf pulse β. Circles mark the experimental data, the line shows the theoretically expected curve.

tions is of fundamental interest, as such fields offer new ways of studying the relative translational diffusion of atoms, chaotic spin dynamics, and multiple quantum coherences in simple systems close to an ideal gas [12,25,26]. Such experiments are made possible by exploiting high spin polarizations not only for increasing the NMR signal, but also to dramatically shorten the time required for the formation of IMQCs. In free gases diffusion can be controlled by buffer gases; in porous media DDFs will provide unique information about diffusion in the sample itself. Indeed, the usefulness of IDQCs for the study of such systems was already shown for liquids and gases with densities comparable to liquids [7,12]. In comparison to liquids, LP gases allow the investigation of larger structures over a bigger range of pore sizes, as the dipolar coupling distance exceeds the one in liquids and can be varied easily by changing the amount of polarization. The extreme sensitivity of IDQCs on D offers unprecedented ways of studying gas diffusion in complex structures where diffusion is slowed down due to a logarithmic distribution of channel dimensions, a field of considerable interest for the physics community. The signal maximum dependence on D and T_2 is ideal for setting a quantum filter for medical magnetic-resonance imaging, e.g., in imaging of the lung with its complex structure of a large range of length scales, which are generally characterized by local distributions of diffusion coefficients.

We thank the group of W. Heil for providing the LP ^{3}He, M. Hehn and H. Raich for their help in the design and construction of the gas handling system, and P. Blümler, L. Agulles-Pedrós, and O. L. Mensio for their support during the experiments and fruitful discussions. Financial support from the Deutsche Forschungsgemeinschaft (No. FOR474) and the Consejo Nacional de Investigaciones Científicas y Técnicas of Argentina (CONICET) is also gratefully acknowledged.

*spiess@mpip-mainz.mpg.de

[1] W. S. Warren, W. Richter, A. H. Andreotti, and B. T. Farmer, II, Science **262**, 2005 (1993).
[2] Q. He, W. Richter, S. Vathyam, and W. S. Warren, J. Chem. Phys. **98**, 6779 (1993).
[3] S. Lee, W. Richter, S. Vathyam, and W. S. Warren, J. Chem. Phys. **105**, 874 (1996).
[4] J. Jeener, J. Chem. Phys. **112**, 5091 (2000).
[5] W. S. Warren, S. Ahn, M. Mescher, M. Garwood, K. Ugurbil, W. Richter, R. R. Rizi, J. Hopkins, and J. S. Leigh, Science **281**, 247 (1998).
[6] J. Zhong, Z. Chen, E. Kwok, and S. D. Kennedy, Magn. Reson. Imaging **19**, 33 (2001).
[7] L. S. Bouchard and W. S. Warren, J. Magn. Reson. **170**, 299 (2004).
[8] J. Granwehr, J. T. Urban, A. H. Trabesinger, and A. Pines, J. Magn. Reson. **176**, 125 (2005).
[9] A. Schafer and H. E. Moller, Magn. Reson. Med. **58**, 696 (2007).
[10] I. Ardelean and R. Kimmich, J. Chem. Phys. **112**, 5275 (2000).
[11] Z. Chen and J. Zhong, J. Chem. Phys. **114**, 5642 (2001).
[12] J. Baugh, A. Kleinhammes, D. Han, Q. Wang, and Y. Wu, Science **294**, 1505 (2001).
[13] P. P. Zanker, J. Schmidt, J. Schmiedeskamp, R. H. Acosta, and H. W. Spiess, Phys. Rev. Lett. **99**, 263001 (2007).
[14] R. H. Acosta, L. Agulles-Pedros, S. Komin, D. Sebastiani, H. W. Spiess, and P. Blumler, Phys. Chem. Chem. Phys. **8**, 4182 (2006).
[15] E. L. Hahn, Phys. Rev. **80**, 580 (1950).
[16] Z. Chen, S. Zheng, and J. Zhong, Chem. Phys. Lett. **347**, 143 (2001).
[17] J. P. Marques, S. Grant, S. Blackband, and R. W. Bowtell, J. Chem. Phys. **123**, 164311 (2005).
[18] W. Richter, S. Lee, W. S. Warren, and Q. He, Science **267**, 654 (1995).
[19] S. Vathyam, S. Lee, and W. Warren, Science **272**, 92 (1996).
[20] W. Richter and W. S. Warren, Concepts Magn. Reson. **12**, 396 (2000).
[21] J. M. Wild, J. Schmiedeskamp, M. N. J. Paley, F. Filbir, S. Fichele, L. Kasuboski, F. Knitz, N. Woodhouse, A. Swift, and W. Heil *et al.*, Phys. Med. Biol. **47**, N185 (2002).
[22] J. Jeener, in *Encyclopedia of NMR*, edited by D. M. Grant and R. K. Harris (John Wiley & Sons, Chichester, 2002), Vol. 9, pp. 642–679.
[23] P. P. Zanker, Ph.D. thesis, Johannes Gutenberg-Universitat, Mainz, 2007.
[24] W. Barros, Jr., J. C. Gore, and D. F. Gochberg, J. Magn. Reson. **178**, 166 (2006).
[25] Y.-Y. Lin, N. Lisitza, S. Ahn, and W. S. Warren, Science **290**, 118 (2000).
[26] J. Jeener, J. Chem. Phys. **116**, 8439 (2002).